

Molecular Relaxation Dynamics of Self-Assembled Monolayers

Qing Zhang, Qiang Zhang, and Lynden A. Archer*

School of Chemical and Biomolecular Engineering, Cornell University, Ithaca, New York 14853-5201

Received: January 13, 2006

Dielectric relaxation spectroscopy is used to quantify molecular motion in alkylsilane SAMs coated on porous glass over a broad temperature range, -30 to -150 °C. Systematic measurements using SAMs with variable coating densities allow us to determine the effect of monolayer disorder on molecular mobility in thin molecular films. A relaxation process with an activation energy of ~ 25 kJ/mol is found to dominate dynamics of SAM-chain segments near the substrate. By introducing polar CN groups at the ends of the chain, we show that the relaxation process in the monolayer canopy can be isolated and studied. This approach can be generalized to other substituent polar groups to probe localized relaxation dynamics in surface-grafted monolayer films.

Introduction

Monomolecular coatings produced by molecular self-assembly are among the most widely used materials for scientific research today. These materials are routinely employed for manipulating the interfacial chemistry, charge transport, and physical properties of solid surfaces.^{1,2} The popularity of self-assembled monolayers (SAMs) is easily traced to their chemical flexibility and to the potential they provide for exerting molecular-level control over the structure and chemistry of surfaces. A large volume of, primarily, experimental research has been devoted to understanding how intermolecular and molecular–substrate interactions affect the structures of SAMs and to determining how the orientation and conformational order in these coatings influence surface physical properties, such as friction, wetting, and adhesion.^{3–5}

Surface-force-apparatus (SFA) and lateral-force-microscopy (LFM) studies on thin molecular films suggest that the mobility of grafted molecules in these films is strongly correlated with their interfacial friction properties.^{6,7} The relaxation dynamics of molecules in SAMs are also widely believed to play an important role in transport processes related to conductivity, adhesion, and the dynamic wetting of substrates functionalized with SAMs.^{8,9} The dynamic properties of alkyl chains at surfaces have also been argued to control the temperature-dependent phase behavior of thin molecular films.^{8,10} Silica gel coated with alkylsilane SAMs are widely used as stationary phases in liquid chromatography (LC), and solid-state NMR studies^{11,12} indicate that the structure and mobility of grafted alkyltrichlorosilane is strongly correlated with the efficiency and selectivity of separations. Because of the growing realization that the motion of single molecules and molecular assemblies in a thin film strongly influences its thermal, mechanical, and electronic transport properties, computer simulations have been used to study the structure and dynamics of SAMs on planar substrates,¹³ whereas experimentally obtained information on molecular motions in SAMs has proven quite elusive. This situation can be traced to multiple factors. The low signal levels ($\sim 10^{-10}$ mol materials) produced by SAM coatings on planar surfaces prevent the application of standard measurement techniques such

as nuclear magnetic resonance that are conventionally used to probe molecular relaxation processes in materials.⁸

Fortunately, it is possible in some situations to scale-up the substrate surface area by several orders of magnitude using nanoparticles or nanoporous materials. Using this approach, local chain ordering and dynamics of self-assembled monolayers on these substrates have been studied via FTIR spectroscopy, differential scanning calorimetry (DSC), and solid-state NMR.^{11,12,14–18} A ^2H NMR line shape analysis, for example, indicates that despite the presence of a strong sulfur–gold surface bond and significant interchain interactions, tethered alkanethiolate chains can still execute rapid trans-gauche bond isomerizations and axial chain rotations.^{14,15} Furthermore, ^{13}C -longitudinal relaxation time ($T_{1\rho}$) data show that even close-packed alkyl chains in an alkylsilane SAM can manifest large-amplitude motions at ambient temperature.^{11,12} But the interpretation of dynamic NMR data is complicated and, in general, a dynamic model is needed to extrapolate the quantitative information from the measurement, and it is difficult to obtain detailed and quantitative information about the molecular motion in those SAMs, such as the time- and length-scales on which it occurs and their dependence on temperature. Therefore, there is a need to find an alternative, more accessible experimental tool to probe the dynamic properties of monolayers.

Dielectric relaxation spectroscopy (DRS) is a sensitive measurement technique for probing molecular relaxation processes on a wide range of time scales.¹⁹ This method characterizes molecular scale dynamics through its relationship to transient changes in the dielectric properties of a macroscopic sample that occur when the sample is excited by a time-dependent electric field. Measurements of the resulting polarization, expressed by the frequency-dependent complex permittivity (ϵ^*) and conductivity (σ), therefore provide a useful method for characterizing both the amplitude and time scale of charge-density fluctuations within the sample. Such fluctuations generally arise from the reorientation of permanent dipole moments of individual molecules or from the rotation of dipolar moieties in flexible molecules such as polymers. The measurement frequency of DRS ranges from 10^{-4} to 10^{12} Hz, which makes it a powerful technique to probe dynamic processes over a wide range of time scales.

DRS has been widely used to investigate the relaxation processes of both polymers and small molecules possessing

* To whom correspondence should be addressed. E-mail: laa25@cornell.edu.

permanent dipole moments.¹⁹ Recently, it has been applied to study the dynamic behavior of glass forming liquids and liquid crystals confined in porous matrices.^{20–22} In this article, DRS is used for the first time ever to study dynamic properties of alkylsilane SAMs tethered to controlled porous glass (CPG) substrates. These measurements yield quantitative information about the molecular relaxation processes in SAMs, making it possible to explore the molecular mechanisms of motion in these coatings.

Experimental Section

Preparation of SAMs. *N*-decyltrichlorosilane($\text{CH}_3(\text{CH}_2)_9\text{SiCl}_3$), *n*-octadecyltrichlorosilane ($\text{CH}_3(\text{CH}_2)_{17}\text{SiCl}_3$), and 11-cyanoundecyltrichlorosilane ($\text{NC}(\text{CH}_2)_{11}\text{SiCl}_3$) were purchased from Gelest and used as received. Toluene and methylene chloride were HPLC-grade and purchased from Aldrich Chemicals. CPG powders (Millipore), which have large surface-to-volume ratios ($141 \text{ m}^2/\text{g}$) with 12.8 nm pore sizes and narrow pore size distributions ($\pm 5.1\%$), were heated at 380 °C for 5 h to remove adsorbed water and organic impurities and then stored in air. The CPG powders were degassed at 95 °C for 3 h just before performing the coating reaction.

SAMs were attached to CPG using the following protocol: 0.2 g CPG was dispersed in 50 mL toluene, and the resulting mixture was sonicated for 20 min. To produce SAM coatings with variable grafting densities, predetermined amounts (50 μL to 5 mL) of octadecyltrichlorosilane ($\text{C}_{18}\text{H}_{37}\text{SiCl}_3$) was added to the continuously stirred air-free suspension and the reaction allowed to proceed for 48 h at room temperature. The unreacted surfactant was removed by successive washes and centrifugation with toluene. The coated CPG was then washed with methylene chloride and dried in a vacuum for 48 h.

Elemental Analysis. Elemental analyses of all of the coatings were carried out by Desert Analytics Inc., Tucson, AZ. The percentage of carbon in the coatings was measured by a Perkin-Elmer 2400 CHN analyzer and was used to calculate the surface coverage of the coatings.

Fourier Transform Infrared Spectroscopy (FTIR). FTIR spectroscopy was collected on a Bruker Equinox 55 Fourier transform spectrometer. The measurements were performed at room temperature with KBr pellets. Each pellet contained 2 mg of coated CPG powders and 100 mg of KBr. Spectra were collected in the transmission mode with an unpolarized beam at a resolution of 4 cm^{-1} with 64 scans. The frequencies of the methylene symmetric and antisymmetric stretching vibrations, which are sensitive to the conformation of alkyl chains in the SAMs, were recorded for all samples studied.

Dielectric Relaxation Spectroscopy (DRS). All DRS experiments were performed using a commercial Novocontrol BDS-80 broadband dielectric spectrometer in the frequency range $1\text{--}10^7 \text{ Hz}$ and at temperatures from -30 to $-150 \text{ }^\circ\text{C}$. The samples, packed into pellet shapes, were sandwiched between two gold-plated copper disks (diameter 20 mm), and the temperature was controlled by a liquid-nitrogen stream. Before the measurements were taken, the samples were first held at 120 °C for 1 h to remove any adsorbed moisture. A comparison of the IR spectra of a sample before and after heating shows no difference in the alkyl chain conformations. The effect of this treatment was manifested by the reduced intensity of the low-frequency conductivity contribution to the dielectric loss as compared with those of nonheated samples.

In the experiments, the complex dielectric permittivity

$$\epsilon^*(\nu) = \epsilon'(\nu) - i\epsilon''(\nu) \quad (1)$$

given by the one-sided Fourier transform of the time derivative

TABLE 1: Properties of C18 SAMs on CPG

concentration of OTS (V/V)	elemental analysis (%C)	coating density ($\mu\text{mol}/\text{m}^2$)	$\nu_a(\text{CH}_2)^a$ (cm^{-1})	$\nu_s(\text{CH}_2)^b$ (cm^{-1})
1.00%	16.35	6.41	2922.9	2853.3
0.20%	15.03	5.80	2923.8	2854.0
0.12%	13.41	5.07	2924.2	2854.3
0.10%	11.31	4.19	2926.6	2856.7

^a Antisymmetric methylene-band positions. ^b Symmetric methylene-band positions.

of the dipole–dipole correlation function $C(t)$ was measured. Here, ν is the frequency of the electric field, $\epsilon'(\nu)$ is the dynamic dielectric constant, and $\epsilon''(\nu)$ is the dielectric loss, which is related to molecular dipole relaxation.

Results and Discussion

CH_3 -Terminated SAMs. Previous work on the preparation of alkylsilane coatings on silica colloids and gels shows that the pretreatment of silica substrates has an important influence on film structure, which is attributed to different amounts of water adsorbed on the silica surface.²³ Some traces of water, that is, a monolayer, adsorbed onto silica surfaces are essential for obtaining alkylsilane monolayers with high coverage; however, the presence of too much water results in the formation of a multilayer. In this work, the standard procedure proposed by Margel and co-workers was adopted to prepare reproducible alkylsilane coatings with uniform monolayer structures.²³ The surface coverage of the coatings prepared in this way was measured by elemental analysis, and the results are shown in Table 1 for CPG reacted with different concentrations of octadecyltrichlorosilane (OTS). It is apparent from these results that grafting density increases as the concentration of OTS increases, and the highest grafting density that can be obtained using the current procedure is $6.4 \mu\text{mol}/\text{m}^2$, which is lower than that for fully ordered 2D SAMs on planar surfaces ($\sim 8.1 \mu\text{mol}/\text{m}^2$), and this suggests the coatings are essentially monolayers or partial monolayers.^{1,24} The methylene symmetric $\nu_s(\text{CH}_2)$ and antisymmetric vibrational frequencies $\nu_a(\text{CH}_2)$ detected by FTIR are also shown in Table 1. These frequencies are known to be related to the population of trans and gauche conformers in the alkyl chains. For all trans chains, $\nu_s(\text{CH}_2)$ is typically around 2850 cm^{-1} and $\nu_a(\text{CH}_2)$ around 2918 cm^{-1} , and for liquid-like disordered chains they are around 2856 and 2928 cm^{-1} , respectively.^{14,25} It can be seen from Table 1 that even for OTS SAMs with the highest coating density, $\nu_s(\text{CH}_2)$ and $\nu_a(\text{CH}_2)$ are at 2953 and 2923 cm^{-1} respectively, indicating a less ordered structure compared with that of SAMs on planar surfaces. As revealed in previous FTIR and NMR studies of alkylsilane SAMs on porous silica surfaces,^{24,26} the high radius of curvature and local roughness of the porous materials lead to a lower packing density and a more disordered structure of SAMs, which may result in faster relaxation dynamics. Table 1 also shows that as the surface coverage decreases the two peak positions shift to higher frequencies, indicating that the SAMs possess a more disordered structure. This result suggests that for monolayers with low grafting density, a homogeneous low-density coating is more plausible than islands of densely packed ordered chains.

Figure 1 shows the dielectric loss spectra at selected temperatures for OTS-coated CPG with two different grafting densities. It is apparent from Figure 1a that a measurable relaxation maximum is observed at high frequencies, and the maximum simultaneously moves to lower frequencies and broadens as the temperature decreases. Control experiments

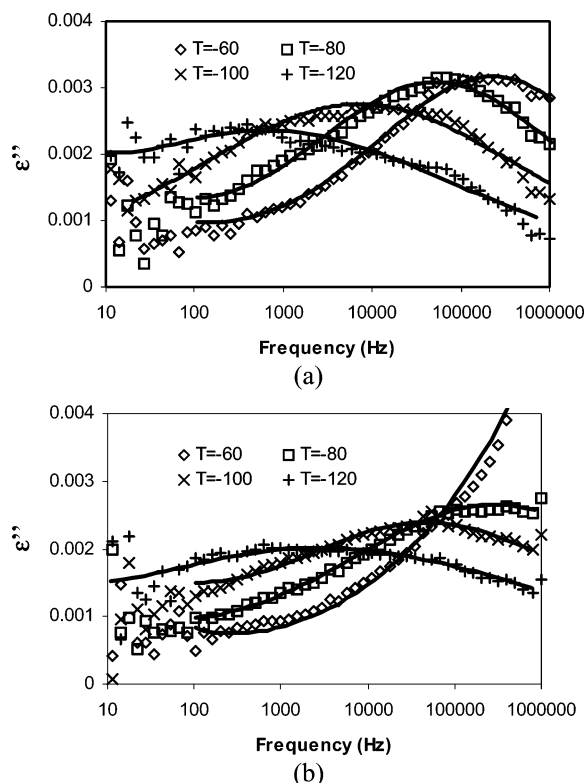


Figure 1. Dielectric loss $\epsilon''(\nu)$ vs frequency at selected temperatures ($^{\circ}\text{C}$) for C18 methyl-terminated SAMs on CPG with coating densities of (a) $d = 6.41 \mu\text{mol}/\text{m}^2$ and (b) $d = 5.48 \mu\text{mol}/\text{m}^2$. The scattered symbols represent experimental data, and the solid lines represent fits to the data according to Havriliak–Negami functions. The measurement errors in the dielectric spectra are smaller than the symbols for the data.

performed using bare CPG samples show no relaxation peaks in the dielectric loss spectra, indicating that the observed loss peak is associated with molecular segment relaxation in the grafted monolayers. It can be seen from Figure 1b that as grafting density decreases the loss peak becomes less intense and, at fixed temperatures, moves to higher frequencies. This finding suggests that the relaxation processes responsible for the dielectric loss peak become faster as coating density decreases. At an even lower grafting density (less than $2 \mu\text{mol}/\text{m}^2$), no peak can be resolved because of the large noise-to-signal ratio.

To extract quantitative information about relaxation motions, the dielectric spectra were fitted to the empirical Havriliak–Negami (HN) function (see Figure 1)

$$\epsilon^*(\nu) = \frac{\Delta\epsilon}{(1 + (2\pi\nu\tau)^{\alpha})^{\beta}} + \epsilon'(\nu \rightarrow \infty) \quad (2)$$

The first term on the right describes the dielectric relaxation with a characteristic relaxation time τ and a dielectric relaxation strength $\Delta\epsilon$, where α and β are parameters that account for the symmetrical and asymmetrical broadening of the relaxation peak, respectively. The contribution of dc conductivity to dielectric loss is negligible because the samples are well dried and the measurements performed at low temperatures ($T \leq -30^{\circ}\text{C}$). The relaxation times τ (s) determined using the above procedure for OTS SAMs with a range of coating densities are plotted as a function of temperature in Figure 2. It is clear from the plot that at a fixed temperature, SAMs with lower grafting densities display faster relaxation dynamics. FTIR data for these same materials (Table 1) indicate that alkyl chains are more

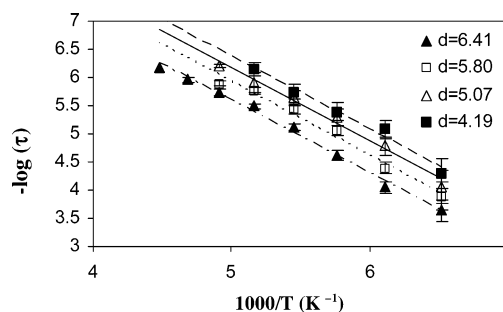


Figure 2. Temperature dependence of relaxation times for C18 SAMs with different coating densities d ($\mu\text{mol}/\text{m}^2$). Straight lines correspond to the Arrhenius fit.

TABLE 2: Shape Parameter α for C18 SAMs at Different Temperatures^a

density ($\mu\text{mol}/\text{m}^2$)	α			
	$T = -30^{\circ}\text{C}$	$T = -60^{\circ}\text{C}$	$T = -90^{\circ}\text{C}$	$T = -120^{\circ}\text{C}$
5.80	0.53 ± 0.05	0.51 ± 0.05	0.48 ± 0.05	0.27 ± 0.05
5.07	0.43 ± 0.05	0.41 ± 0.05	0.35 ± 0.05	0.25 ± 0.05

^a α is the shape parameter that characterizes the symmetrical broadening of relaxation peaks.

TABLE 3: Activation Energy for C18 SAMs on CPG

density ($\mu\text{mol}/\text{m}^2$)	6.41	5.80	5.07	4.19
ΔE (kJ/mol)	24.6	24.9	25.0	24.9

disordered at lower densities, providing a straightforward explanation for these observations. The values of the shape parameter α , which characterizes the broadening of the relaxation peak, is listed in Table 2 for C18 SAMs at different temperatures. It can be seen that the values of α are less than 1 ($\alpha = 1$ corresponding to a Debye type relaxation) and become smaller at lower temperatures. This indicates a distribution of relaxation time rather than a single relaxation mode, and the distribution becomes broader as temperature decreases.

To gain more insight into the mechanism of the observed relaxation process, it is instructive to compare it with the relaxation behavior of linear polyethylene (PE), which possesses a backbone structure similar to that of the SAMs. It is known that there are three prominent relaxation processes (α , β , and γ in order of descending temperature) for linear polyethylene.^{27,28} Previous studies show that at a comparable temperature range, the γ relaxation of linear PE is in a frequency range similar to that of the relaxation process reported here for SAMs.^{27–30} Reported values for the activation energy of the γ process for PE range from 10 to 60 kJ/mol. It is believed that this range reflects the fact that the γ process is itself a superposition of several local relaxation modes, including rapid trans-gauche transitions ($\Delta E \sim 10$ to 20 kJ/mol), the axial chain rotation, and the reorientation motion of short (e.g., two to three methylene groups) alkyl chain segments ($\Delta E \sim 20$ to 60 kJ/mol).^{27,29,30} The activation energy ΔE for the relaxation process of SAMs can be estimated from the slope of the Arrhenius plot in Figure 2, and the results are shown in Table 3. A comparison of the activation energies shows that the ΔE value of SAMs (~ 25 kJ/mol) is somewhat higher than that of the trans-gauche conformation transition, indicating that the localized C–C bond rotation is likely not the principal relaxation mechanism probed by the dielectric measurements on SAMs. The ΔE value of SAMs is in the range of the ΔE values reported for the other two γ processes in polyethylene. Also, the generally lower packing density of alkyl chains in SAMs coated on porous glass ($\rho < 0.81 \text{ g}/\text{m}^3$) relative to that of linear PE ($\rho > 0.90 \text{ g}/\text{m}^3$)²⁹ means that the measured activation energy is likely an

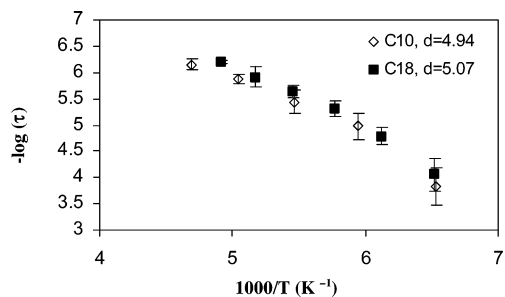


Figure 3. Arrhenius plot of relaxation times for C10 and C18 SAMs with similar coating densities.

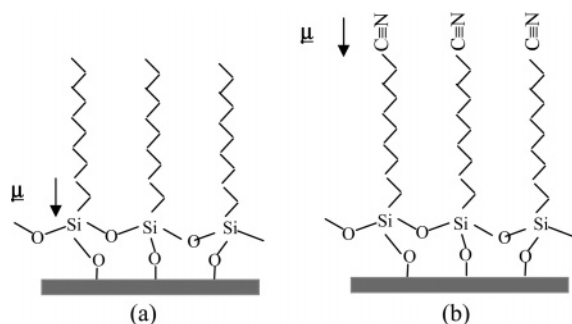


Figure 4. Dipole moments (μ) in (a) CH_3 - and (b) CN-terminated SAMs.

underestimate. We therefore tentatively conclude that the relaxation dynamics evident from the dielectric loss spectra reflect the reorientation motion of short stretches of alkyl chain segments near the substrate (see below).

Alkylsilane SAMs composed of shorter chain molecules ($\text{CH}_3(\text{CH}_2)_9\text{SiCl}_3$) were prepared using similar methods, and their dielectric properties were studied by DRS. Figure 3 provides a comparison of relaxation times for C10 SAM and C18 SAM at comparable grafting densities. It can be seen that the two curves are indistinguishable over the temperature range studied. This result indicates that the dominant relaxation process is the same for the two SAMs despite their large difference in carbon chain length, confirming that the observed relaxation process is a localized one involving only a few (certainly less than 10) carbons.

CN-Terminated SAMs. It is well known that alkyl chains are not inherently dielectric active.^{27,28} That alkyl chain SAMs manifest a measurable dielectric relaxation is, however, unsurprising. The three polar Si–O bonds at the head of grafted molecules may produce a strong localized dipole that can induce a weaker dipole in a short run of segments near the molecule–substrate interface (Figure 4). On the basis of the observations outlined above, we believe this dipole is the likely source of the observed relaxation process. It therefore follows that if a strong dipole can be introduced at any other location in the SAM, it should be possible to exploit the inherently weak dielectric activity of alkyl chains to probe relaxation dynamics at these locations using the introduced dipole. To test this idea, SAMs composed of cyano-terminated alkylsilane ($\text{NC}(\text{CH}_2)_{11}\text{SiCl}_3$) were coated on porous glass, and their relaxation dynamics were quantified using DRS (Figure 5). It is readily apparent from Figure 5a that the introduction of polar CN functional groups to the chain ends of each grafted molecule leads to a nearly 10-fold increase in dielectric loss amplitude. The shifting of loss maxima and the broadening of the dielectric loss spectrum with reducing temperature are also now quite apparent from the plot. This approach therefore provides a powerful new method for probing the relaxation dynamics of

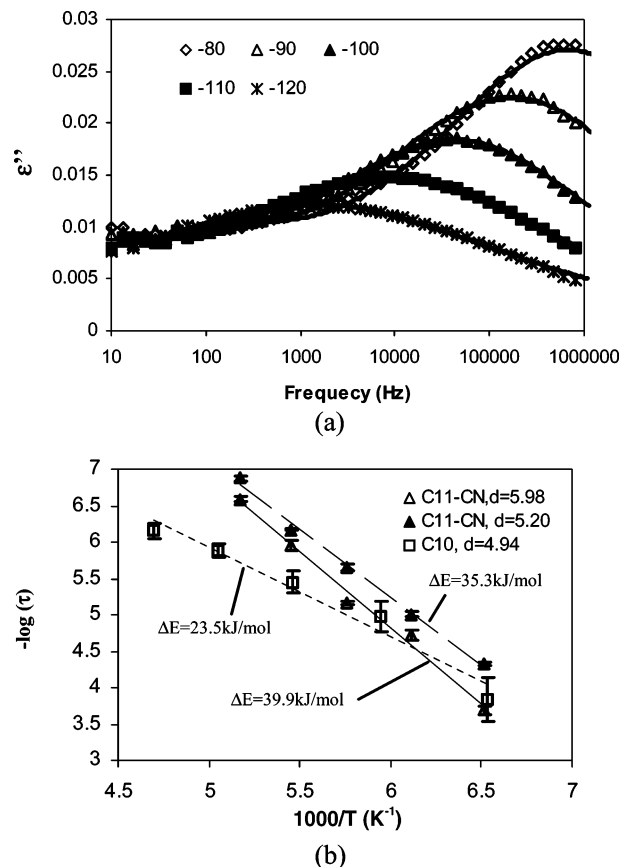


Figure 5. Typical dielectric loss spectra of CN-terminated SAMs (coating density: $5.53 \mu\text{mol}/\text{m}^2$) (a); Arrhenius plot of relaxation time for CN-terminated SAMs, compared with CH_3 -terminated SAMs with similar chain lengths and coating densities (b).

localized sections of tethered alkyl chains as well as for isolating component dynamics in mixed SAMs or in SAMs designed using architecturally complex molecules.

The temperature dependence of the relaxation time for CN-terminated SAMs is compared with CH_3 -terminated SAMs of comparable chain lengths and grafting densities in Figure 5b. It is again immediately apparent from the plot that at comparable temperatures the relaxation process of the CN-terminated SAMs is much faster, but the activation energies are generally higher than that of CH_3 -terminated SAMs. The relaxation times and activation energies for CN-terminated SAMs are also generally lower for coatings with lower grafting densities. Because the relaxation process observed for CH_3 -terminated SAMs is believed to be associated with the local motions of a short segment near the substrate, it is likely that the relaxation process observed for the CN-terminated SAMs arises from similar motions of molecular segments near the chain end (SAM canopy). A previous FTIR study of specifically deuterated alkylthiol SAMs on gold nanoparticles revealed that the segments near the chain ends possess a more disordered structure compared with that of the inner segments.^{8,14} Even though it is not clear how the polar end groups affect intermolecular interactions in the monolayer, the shorter relaxation times for this process is consistent with the IR results, suggesting that the chain ends possess a more disordered structure, and hence have a higher mobility than the segments localized in the highly ordered region near the substrate. Given the greater disorder in the SAM canopy, reorientation or rotation processes near the chain ends will likely involve a larger number of molecular segments, which will lead to a higher overall activation energy

for this process, which is consistent with what was observed. It is nonetheless clear that in either case (dipoles near the substrate or in the SAM canopy) only a fraction of each SAM chain is involved in the measured relaxation process. Thus even in imperfectly ordered monolayers, intermolecular interactions are strong enough to prohibit a large amplitude motion of entire molecules, and only local motions of short segments are possible.

In summary, we have reported a quantitative experimental study of molecular relaxation in self-assembled monolayers. Two relaxation processes, corresponding to local motions of molecular segments near the chain heads and chain ends respectively, were observed. We have also shown that the selective introduction of polar groups to targeted positions in molecules constituting a monolayer coating can be used to enhance local dielectric responses and isolate the molecular relaxation dynamics of these sections. This procedure is readily applicable to SAMs of varying structures (different chain lengths, architectures, end groups, and compositions of backbones) and to SAMs that manifest more complex intermolecular interactions (e.g., nematics, hydrogen bridges, etc.) to obtain abundant molecular-level information on the structure and dynamics of monolayers.

Acknowledgment. This research was supported by the National Science Foundation Tribology Program (Grant CMS-0004525), the Department of Energy (Nanosciences Program) (Grant DE-FG02-02ER4600), and the Cornell Center for Materials Research, a Science and Engineering Center of the National Science Foundation (DMR-0079992).

References and Notes

- (1) Schreiber, F. *Prog. Surf. Sci.* **2000**, *65*, 151–256.
- (2) Ulman, A. *Chem. Rev.* **1996**, *96*, 1533–1554.
- (3) Lio, A.; Charych, D. H.; Salmeron, M. *J. Phys. Chem. B* **1997**, *101*, 3800–3805.
- (4) Tsukruk, V. V. *Adv. Mater.* **2001**, *13*, 95–108.
- (5) Shon, Y. S.; Lee, S.; Colorado, R.; Perry, S. S.; Lee, T. R. *J. Am. Chem. Soc.* **2000**, *122*, 7556–7563.
- (6) Yoshizawa, H.; Chen, Y. L.; Israelachvili, J. N. *J. Phys. Chem.* **1993**, *97*, 4128–4140.
- (7) Zhang, Q.; Archer, L. A. *J. Phys. Chem. B* **2003**, *107*, 13123–13132.
- (8) Badia, A.; Lennox, R. B.; Reven, L. *Acc. Chem. Res.* **2000**, *33*, 475–481.
- (9) Badia, A.; Back, R.; Lennox, R. B. *Angew. Chem., Int. Ed. Engl.* **1994**, *33*, 2332–2335.
- (10) Sandhyarani, N.; Pradeep, T. *Int. Rev. Phys. Chem.* **2003**, *22*, 221–262.
- (11) Pursch, M.; Sander, L. C.; Egelhaaf, H. J.; Raitza, M.; Wise, S. A.; Oelkrug, D.; Albert, K. *J. Am. Chem. Soc.* **1999**, *121*, 3201–3213.
- (12) Pursch, M.; Vanderhart, D. L.; Sander, L. C.; Gu, X.; Nguyen, T.; Wise, S. A.; Gajewski, D. A. *J. Am. Chem. Soc.* **2000**, *122*, 6997–7011.
- (13) Hautman, J.; Klein, M. L. *J. Chem. Phys.* **1989**, *91*, 4994.
- (14) Badia, A.; Cuccia, L.; Demers, L.; Morin, F.; Lennox, R. B. *J. Am. Chem. Soc.* **1997**, *119*, 2682–2692.
- (15) Schmitt, H.; Badia, A.; Dickson, L.; Reven, L.; Lennox, R. B. *Adv. Mater.* **1998**, *10*, 475–480.
- (16) Voicu, R.; Badia, A.; Morin, F.; Lennox, R. B.; Ellis, T. H. *Chem. Mater.* **2001**, *13*, 2266–2271.
- (17) Zeigler, R. C.; Maciel, G. E. *J. Am. Chem. Soc.* **1991**, *113*, 6349.
- (18) Pursch, M.; Sander, L. C.; Albert, K. *Anal. Chem.* **1996**, *68*, 4107.
- (19) Hill, N. E.; Vaughan, W. E.; Price, A. H.; Davies, M. *Dielectric Properties and Molecular Behaviour*; Van Nostrand Reinhold Press: London, 1969.
- (20) Arndt, M.; Stannarius, R.; Groothues, H.; Kremer, F. *Phys. Rev. E: Stat. Phys., Plasmas, Fluids, Relat. Interdiscip. Top.* **1996**, *54*, 5377–5390.
- (21) Cramer, C.; Cramer, T.; Kremer, F.; Stannarius, R. *J. Chem. Phys.* **1997**, *106*, 3730–3742.
- (22) Aliev, F. M.; Nazario, Z.; Sinha, G. P. *J. Non-Cryst. Solids* **2002**, *305*, 218–225.
- (23) Brandriss, S.; Margel, S. *Langmuir* **1993**, *9*, 1232.
- (24) Gao, W.; Reven, L. *Langmuir* **1995**, *11*, 1860–1863.
- (25) MacPhail, R. A.; Strauss, H. L.; Snyder, R. G.; Elliger, C. A. *J. Phys. Chem.* **1984**, *88*, 334–341.
- (26) Srinivasan, G.; Pursch, M.; Sander, L. C.; Muller, K. *Langmuir* **2004**, *20*, 1746–1752.
- (27) Ashcraft, C. R.; Boyd, R. H. *J. Polym. Sci.* **1976**, *14*, 2153–2193.
- (28) Sayre, J. A.; Swanson, S. R.; Boyd, R. H. *J. Polym. Sci.* **1978**, *16*, 1739–1759.
- (29) Khanna, Y.; Turi, E. A.; Taylor, T. J. *Macromolecules* **1985**, *18*, 1302–1309.
- (30) Matsuo, M.; Bin, Y.; Xu, C.; Ma, L.; Nakaoki, T.; Suzuki, T. *Polymer* **2003**, *44*, 4325–4340.